GLOBAL BIOGEOCHEMICAL CYCLES, VOL. 27, 941–949, doi:10.1002/gbc.20081, 2013

Prevalence of strong vertical CO_2 and O_2 variability in the top meters of the ocean

Maria Ll. Calleja,[1,2] Carlos M. Duarte,[1,3] Marta Álvarez,[4] Raquel Vaquer-Sunyer,[5] Susana Agustí,[1,3] and Gerhard J. Herndl[6,7]

Received 5 February 2013; revised 28 June 2013; accepted 1 August 2013; published 13 September 2013.

[1] The gradient in the partial pressure of carbon dioxide (pCO_2) across the air-sea boundary layer is the main driving force for the air-sea CO_2 flux. Global data bases for surface seawater pCO_2 are actually based on pCO_2 measurements from several meters below the sea surface, assuming a homogeneous distribution between the diffusive boundary layer and the upper top meters of the ocean. Compiling vertical profiles of pCO_2, temperature, and dissolved oxygen in the upper 5–8 m of the ocean from different biogeographical areas, we detected a mean difference between the boundary layer and 5 m pCO_2 of 13 ± 1 µatm. Temperature gradients accounted for only 11% of this pCO_2 gradient in the top meters of the ocean; thus, pointing to a heterogeneous biological activity underneath the air-sea boundary layer as the main factor controlling the top meters pCO_2 variability. Observations of pCO_2 just beneath the air-sea boundary layer should be further investigated in order to estimate possible biases in calculating global air-sea CO_2 fluxes.

Citation: Calleja, M. Ll., C. M. Duarte, M. Álvarez, R. Vaquer-Sunyer, S. Agustí, and G. J. Herndl (2013), Prevalence of strong vertical CO_2 and O_2 variability in the top meters of the ocean, *Global Biogeochem. Cycles*, *27*, 941–949, doi:10.1002/gbc.20081.

1. Introduction

[2] The quantification and understanding of processes controlling the air-sea exchange of carbon dioxide (CO_2) is critical on determining the global carbon budget and its future evolution on a global climate change scenario [*Fung et al*., 2005; *Gruber et al*., 2009; *Le Quéré et al*., 2010; *McKinley et al*., 2011]. The air-sea CO_2 flux is mainly determined by changes in surface oceanic partial pressure of CO_2 (pCO_2), which varies spatially and temporally between 150 and 550 µatm [*Takahashi et al*., 2009], about 60% below and 30% above the mean atmospheric pCO_2 of 394 µatm (annual mean for 2012, from Mauna Loa records).

[3] Over the last decade, major concerted efforts have been made to assemble a global surface water pCO_2 data set. Currently, two data sets capturing seasonal and geographical variability have been recently released to the public: the LDEO database [*Takahashi et al*., 2012] with about 6.4 million measurements from 1957 to 2011 and the Surface Ocean CO_2 Atlas (SOCAT) database [*Pfeil et al*., 2013] with 6.3 million measurements from 1968 to 2007. Both data sets are largely derived from automated underway systems onboard research vessels and ships of opportunity that are continuously recording the pCO_2 in the overlying marine air and subsurface waters. These systems commonly sample water from 3 to 7 m below the surface, the depth of the intake on the vessel haul [e.g., *Corbière et al*., 2007; *Fung and Takahashi*, 2000; *Inoue et al*., 1996; *Lüger et al*., 2004; *Metzl et al*., 1995; *Murphy et al*., 2001; *Santana-Casiano et al*., 2009], and consider these measurements to be representative of that at the seawater surface by assuming a homogeneous distribution of gases below the air-sea diffusive boundary layer. Thus, the air-sea pCO_2 gradient (ΔpCO_2), which drives the air-sea CO_2 flux, is calculated assuming that pCO_2 is vertically homogeneous within the upper meters of the ocean. However, there is published but limited evidence of pCO_2 vertical variability between the surface microlayer and the bulk subsurface mixed layer in both lakes [*Hari et al*., 2008] and oceans [*Gong et al*., 2007; *Liu et al*. 2008].

[4] Previous examinations of near-surface vertical gradients of CO_2 partial pressure have focused on temperature gradients [*Robertson and Watson*, 1992; *Ward et al*., 2004] and air-sea heat fluxes [*Phillips*, 2004], revealing thermal stratification within the upper meters of the ocean. The presence of a "warm layer skin" [*Fairall et al*., 1996] is commonly observed at low latitudes and low wind speed and mixing regimes. Also a "cool layer skin" [*Donlon et al*., 2002] is persistent on a global basis at wind speeds exceeding 6 m s^{-1}. This small-scale temperature stratification in the upper meters of the ocean already complicates the direct measurements of surface water pCO_2, as the solubility of CO_2 in seawater is strongly temperature

Additional supporting information may be found in the online version of this article.

[1]Department of Global Change Research, Instituto Mediterráneo de Estudios Avanzados, CSIC-UIB, Esporles, Spain.
[2]Instituto Andaluz de Ciencias de la Tierra, CSIC-UGR, Armilla, Spain.
[3]The UWA Oceans Institute, University of Western Australia, Crawley, Western Australia, Australia.
[4]Instituto Español de Oceanografía, Centro de A Coruña, Coruña, Spain.
[5]Department of Geology, Lund University, Lund, Sweden.
[6]Department of Marine Biology, University of Vienna, Vienna, Austria.
[7]Department of Biological Oceanography, Royal Netherlands Institute for Sea Research, Den Burg, Netherlands.

Corresponding author: M. Ll. Calleja, Instituto Andaluz de Ciencias de la Tierra, CSIC-UGR, Avda. de las Palmeras 4, 18100 Armilla, Granada, Spain. (marialluch.calleja@gmail.com)

0886-6236/13/10.1002/gbc.20081

dependent [*Weiss*, 1974; *Takahashi et al*., 1993]. Accordingly, *Ward et al*. [2004] demonstrated that anomalies in air-sea CO_2 fluxes result, at low wind conditions, from variation in the thermal structure of the upper few meters of the ocean. Other studies have also reported significant near-surface temperature gradients even under high wind speed [*Gemmrich and Farmer*, 1999], challenging the homogeneity expected from vertical mixing of the boundary layer. Takahashi and coworkers [*Takahashi et al*., 2009] recently considered the thermal skin effect on pCO_2 to be negligibly small. However, they also recognized the need to examine this and other surface layer effects in order to reduce systematic errors in air-sea pCO_2 differences and consequently in global air-sea CO_2 flux estimates.

[5] In addition to physical processes, seawater pCO_2 in the upper top meters of the ocean has been recently shown to be affected by nonconservative biological processes [*Calleja et al*., 2005; *Ducklow and McCallister*, 2004], and it is well known that the key biological process affecting seawater pCO_2 is the net community production, the net balance between photosynthetic organic carbon fixation, which reduces the partial pressure of CO_2, and respiration of organic matter, which releases CO_2. Hence, pCO_2 vertical variability in the upper meters of the surface layer could also be driven by vertical variability in the net planktonic community metabolism.

[6] During the past decade, significant evidence has been provided pointing to different biochemical and microbial activity and composition in the surface and subsurface layer of different oceanic regions [*Cunliffe et al*., 2013, and references therein]. For example, differences in bacterial diversity (North Sea) [*Franklin et al*., 2005], microbial strains (NW Mediterranean) [*Agogué et al*., 2005], and autotrophic and heterotrophic nanoflagellate abundance (NW Mediterranean) [*Joux et al*., 2006] between surface microlayer and subsurface waters have been reported. These differences in biological diversity and abundance may be related to particulate and dissolved fractions of macronutrients or other biochemically active compounds. For example, *Obernosterer et al*. [2005] identified consistently greater concentrations of particulate organic carbon and nitrogen and of dissolved organic carbon in South Pacific surface microlayer water compared with surface water (5 m). Furthermore, other studies conducted during the 2003 and 2004 cruises where this work was carried out reported significantly higher microbial metabolic rates in the surface microlayer than in the subsurface waters [*Calleja et al*., 2005; *Reinthaler et al*., 2008], which lead to significant differences in CO_2 partial pressure between the two layers and exert a control over the air-sea CO_2 flux [*Calleja et al*., 2005].

[7] Despite evidences, and due to logistics problems, the analysis of the relationship between the evidenced vertical biological heterogeneity and pCO_2 gradients within the upper meters of the water column are scarce, particularly for the open ocean comprising the vast majority of the oceans' surface.

[8] We believe that as the accuracy and precision of surface pCO_2 measurements is increasing [*Körtzinger et al*., 2000], the thermodynamic and biological effects on pCO_2 variability within the upper meters of the surface ocean become even greater potential sources of uncertainty, which can no longer be ignored to accurately assess global air-sea CO_2 fluxes.

[9] In this work, we examine the vertical variability of pCO_2, partial pressure of oxygen (pO_2), and temperature in the upper 5 to 8 m of the ocean from 83 profiles collected between 2003 and 2007 and covering different oceanic biomes. The general aim is to study the vertical homogeneity of pCO_2 in the upper surface meters and also separating thermodynamic effects from biological effects. While changes in temperature lead to parallel changes in pCO_2 and pO_2, since the solubility of both gases is a strong inverse function of seawater temperature, metabolic processes lead to reverse changes in these gases, as a positive net production causes a pCO_2 decrease and a pO_2 increase, while a net negative production (net respiration) leads to higher pCO_2 and lower pO_2.

2. Sampling and Methods

2.1. Location

[10] Our measurements were conducted at 83 stations in four different regions (Figure 1): along the NE subtropical Atlantic Ocean (between 14°W and 32°W, and 19°N and 28°N) during May–June 2003 (cruise COCA-2 on board the R/V Hesperides), September–October 2004 (cruise BADE-2 on board the R/V Pelagia), August–September 2006 (cruise RODA-1 on board the R/V Hesperides), and February 2007 (cruise RODA-2 on board the R/V Hesperides); the Southern Ocean (between 55°W and 70°W, and 62°S and 67°S) during February 2005 (cruise ICEPOS-2 on board of the R/V Hesperides); the Mediterranean Sea and Black Sea (between 7°E and 31°E, and 35°N and 42°N), during June–July 2006 (cruise THRESHOLDS on board the R/V García del Cid); and the Arctic Ocean (between 20°E and 14°W, and 68°N and 81°N) during June–July 2007 (cruise ATOS on board the R/V Hesperides).

2.2. Instrumentation

[11] Vertical profile measurements of CO_2 and O_2 between the top centimeters and 5–8 m depth were performed at 83 open ocean stations from a small pneumatic boat drifting away from any possible contamination source from the research vessel, which could be safely deployed at wind velocities up to 15.7 m s^{-1}.

[12] Determination of water pCO_2 was performed using a high-precision (± 1 ppm) nondispersive infrared gas analyzer (EGM-4, PP-systems) fitted with an electrochemical cell Oxygen probe (OP-2, PP-systems, precision ± 0.02%), averaging measurements at 1 min recording interval. The closed gas stream flowing through the gas (CO_2 and O_2) analyzer was previously equilibrated with the sampled seawater by the use of a peristaltic pump which introduced the seawater into a gas exchange column (MiniModule 1.25 × 9 Membrane Contactor, Celgard) with an effective surface area of 0.5 m^2, total volume of 52 ml, and water flow of about 300 ml min^{-1}, resulting in a residence seawater time of 10 s. Temperature was measured (RTD probe, Fluke, with accuracy and precision of 0.01°C), before (in situ seawater Temperature) and after flowing through the equilibrator, and no temperature difference was detected. Before entering the gas analyzer, the gas stream was circulated through a Calcium Sulfate column to avoid interferences from water vapor.

[13] The gas analyzer was calibrated, in all the cruises, using two dry standards: pure nitrogen (0.0 ppm CO_2) and a gas mixture of CO_2 and N_2 containing a CO_2 molar fraction of 541 ppm, from Carburos Metalicos (Barcelona, Spain), which revealed an accuracy of ± 2 ppm in the determinations of pCO_2

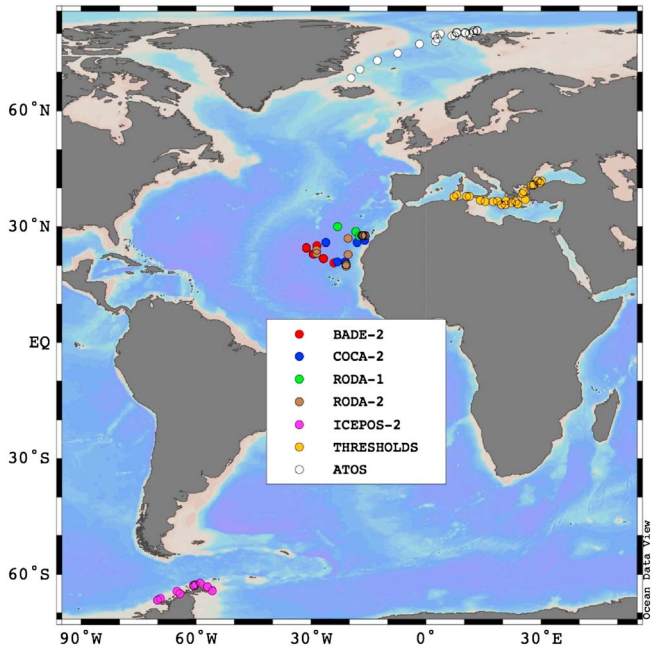

Figure 1. Map showing the location of the stations conducted in different cruises where profiles for pCO_2, O_2 concentration, and temperature were examined within the upper 5 m of the ocean.

measurements. Pure nitrogen gas (0.0% O_2) and pure synthetic air (21.00% O_2) were used for calibration of the Oxygen probe revealing an accuracy of 0.2% in the determinations of pO_2 measurements. Final calculations for pCO_2 and pO_2 were obtained at 1 atmospheric pressure with 100% saturation of water vapor and in situ temperature [*Weiss*, 1974]. Oxygen concentrations (µmol O_2 Kg^{-1}) were calculated from pO_2 (%), temperature, and salinity according to *Benson and Krause* [1984]. O_2 concentrations obtained strongly and significantly correlate ($R^2 = 0.8$, $P < 0.05$) with those measured by the use of the traditional Winkler method (12 parallel measurements, using both methods, were performed during the THRESHOLDS cruise). The results obtained with our method tended to overestimate oxygen concentrations (by, on average, 9 ± 3 µmol O_2 Kg^{-1}) than those obtained by the Winkler method.

[14] The intake of the peristaltic pump was submerged and held in position by a floating device, to measure gases in the top centimeters of the surface. The pump inlet was then progressively lowered allowing gases to equilibrate at each discrete depth where measurements were taken.

[15] Water temperature and salinity profiles from the upper meters were obtained using an Eureka Manta® multiprobe data-logger recording depth and temperature with resolutions of 0.01 m and 0.01°C, respectively, at THRESHOLDS, RODA-1, and RODA-2 cruises. During COCA-2 and ICEPOS-2, temperature profiles could not be obtained, and only discrete measurements at the top centimeters and 5 m depth were available, which were performed within a minute in 1 L flasks with water pumped from these two depths. During BADE-2, temperature profiles, with a resolution of 1 m, were obtained from conductivity, temperature, depth (CTD) casts

Table 1. Number (N) of Observations and Sampling Stations for Each Cruise and Mean ± Standard Error (SE), Minimum (Min) and Maximum (Max) Values Measured for Temperature (T,°C), pCO_2 (µatm), and O_2 Concentration (µmol Kg^{-1}) Within the Top 5 m of the Ocean Surface for Each Cruise

	NE Subtropical Atlantic				Southern Ocean	Mediterranean Sea	Arctic Ocean
Cruise	BADE	COCA	RODA-1	RODA-2	ICEPOS	THRESHOLDS	ATOS
N observations	74	10	22	78	20	130	116
N stations	8	5	4	13	10	23	20
Mean T (°C)	26.46	22.53	24.00	20.63	1.52	21.17	1.76
SE	0.03	0.17	0.14	0.12	0.19	0.17	0.17
Min	25.90	21.60	22.92	18.87	−0.26	18.45	−1.24
Max	27.08	23.24	24.78	22.24	2.18	25.07	5.19
Mean pCO_2 (µatm)	386	347	412	348	327	410	181
SE	2	5	4	2	11	4	3
Min	370	326	384	334	183	309	134
Max	418	372	450	415	375	495	260
Mean O_2 (µmol Kg^{-1})	242.2	299.1	261.1	254.2	241.9	263.5	261.3
SE	1.4	15.3	0.7	0.3	1.5	0.5	0.6
Min	221.8	276.3	256.0	249.5	231.4	252.4	239.9
Max	262.2	343.6	266.5	259.1	254.2	279.5	281.2

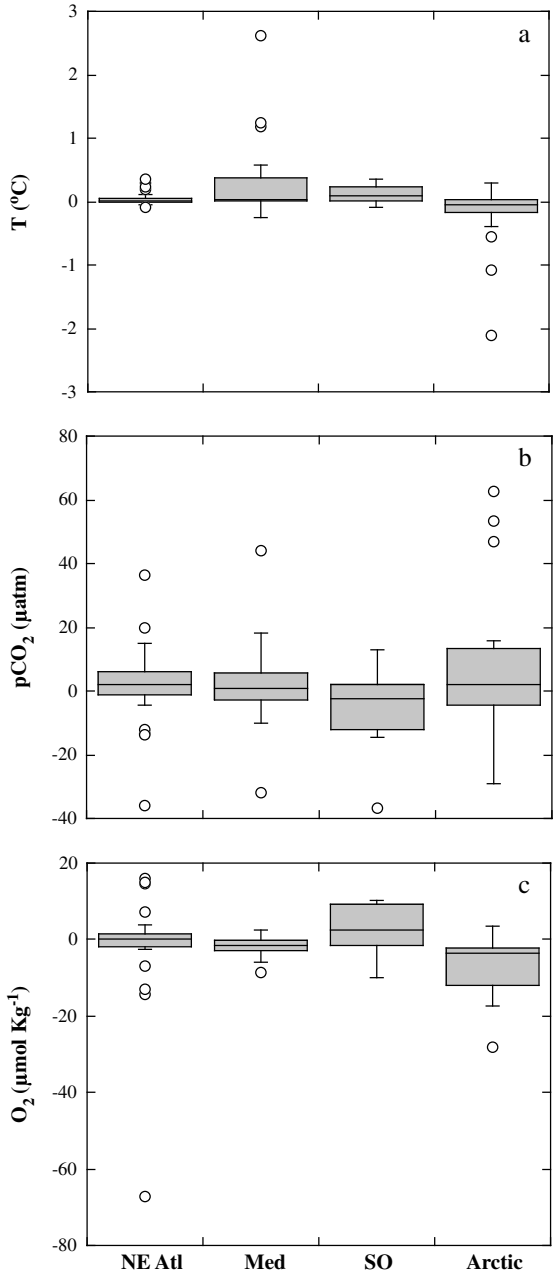

Figure 2. Box plots showing the distribution of the differences between the top centimeters and 5–8 m depth of temperature (°C), pCO_2 (µatm), and oxygen concentration (µmol Kg^{-1}) observed in all different studied regions: North East Subtropical Atlantic (NE Atl), Mediterranean Sea (Med), Southern Ocean (SO), and Arctic Ocean (Arctic). All data from all regions are included. The vertical line in the boxes represents the median, the boxes extend from the 25% to the 75% quartile of the data distribution, and the horizontal lines indicate the 5% and 95% quartiles.

performed from the research vessel at the same time as gas profiles were obtained from the small boat. During ATOS, a Seabird 19 CTD was manually deployed from the small boat and temperature data averaged at 0.5 m intervals.

[16] Wind speed was measured at 1 min intervals using the research vessel equipment: an Aanderaa meteorological station at COCA-2, RODA-1, RODA-2, ICEPOS-2, and ATOS cruises; a Davis Vantage Pro meteorological station at THRESHOLDS cruise; and a Royal Netherlands Meteorological Institute meteo system at BADE-2. Wind speed data were averaged over 60 min prior to the measurements until the end of the sampling period.

[17] Pitch, roll, and heading of the research vessel were also recorded at 1 min intervals and used in a routine embedded in the software integrating navigation and meteorological data to correct wind speed for the ship movement and flow distortion. The corrected wind velocities were then converted to wind at 10 m (U_{10}) using the logarithmic correction $U_{10} = U_z\,[0.097 \ln (z/10) + 1]^{-1}$ where z is the height of the wind sensor position [*Hartman and Hammond*, 1985].

[18] Additional water samples for Chlorophyll *a* (Chl *a*) were collected, for all cruises, using a Rosette sampler system at 5 m depth. Water samples of 150 mL were filtered through 25 mm Whatmann GF/F filters from each station. Collected filters were placed in tubes with a 90% acetone solution for 24 h and extracted Chl *a* was analyzed spectrofluorimetrically on a Shimadzu RF-5301 PC spectrofluorimeter calibrated with pure Chl *a* [*Parsons et al*., 1984]. Surface Chl *a* concentrations were used as a proxy to define the productivity of the different studied areas.

3. Results and Discussion

3.1. Geographical Distribution

[19] Our measurements encompassed a wide range of oceanographic conditions, extending from high-latitude polar regions to lower latitude subtropical waters (see Figure 1). From nutrient-rich and highly productive waters in the Southern and Arctic Oceans (4.7 and 5.6 µg Chl *a* L^{-1}, respectively) to subtropical NE Atlantic Ocean, where conditions ranged from very oligotrophic gyre waters (< 0.1 µg Chl *a* L^{-1}) to productive NW African coast upwelling waters (3.5 µg Chl *a* L^{-1}). Samples from the Mediterranean Sea ranged from 0.1 µg Chl a L^{-1} to 4.2 µg Chl *a* L^{-1}. Overall, sampled surface waters ranged from strongly undersaturated in CO_2 (134 µatm) in the Arctic to highly supersaturated (495 µatm) in the eastern Mediterranean (Black Sea), relative to atmospheric CO_2 concentrations (Table 1). Oxygen concentrations ranged from 221.7 to 343.6 µmol O_2 Kg^{-1}, both observed in the Subtropical Atlantic (Table 1). Water surface Temperature ranged between −1.24°C in polar waters and 27.08°C in subtropical waters (Table 1). Wind speeds, at the time of sampling, ranged from very gentle conditions (0.8 m s^{-1}) to high winds (15.7 m s^{-1}) across the study. Higher wind velocities were reported at the Southern Ocean (mean ± SE, 7.5 ± 1.6 m s^{-1}) and at the NE Atlantic (6.3 ± 0.4 m s^{-1}), whereas the Arctic Ocean and the Mediterranean Sea presented intermediate (5.7 ± 0.5 m s^{-1}) and low (3.6 ± 0.7 m s^{-1}) wind regimes, respectively.

[20] Temperature differences observed between the top centimeters and 5 meters depth were relatively small but above the instrumental error (0.22 ± 0.05°C). However, it was particularly variable in the cruises conducted where lower wind regimes were reported; in the Arctic, where a thin layer of ice melt waters was confined within a near-surface (1–2 m) pycnocline leading to observations with a cold top centimeters layer, and in the Mediterranean Sea, where the upper meters where stratified in the opposite direction (Figure 2a). Overall, in 60% of the data collected, the top centimeters of the ocean were warmer than the waters a few meters below.

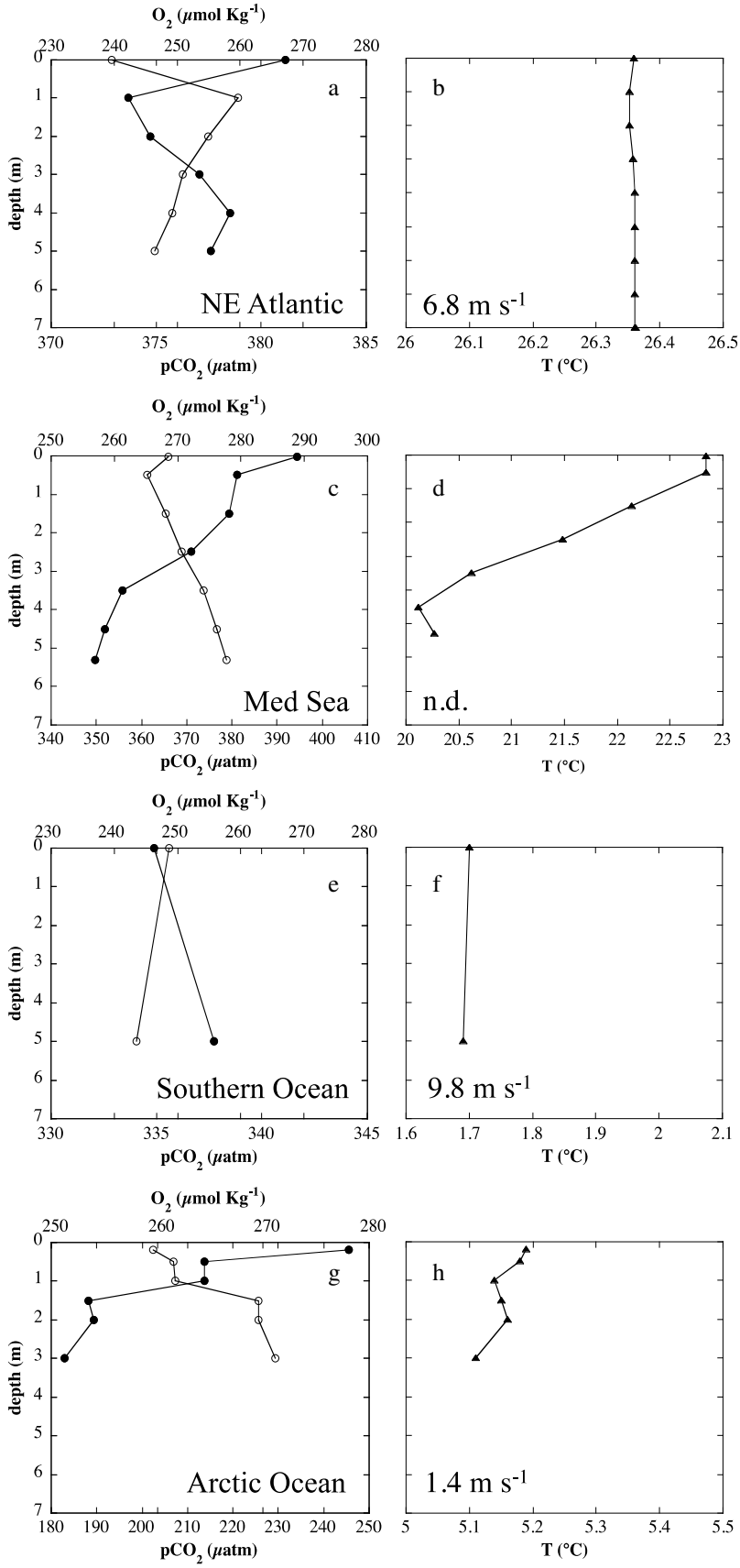

Figure 3. Examples of observed pCO_2 (solid circles), O_2 concentration (open circles), and temperature (solid triangles) vertical profiles within the top meters of the ocean. Wind speed at the time of sampling is shown in insert. n.d. stands for no data.

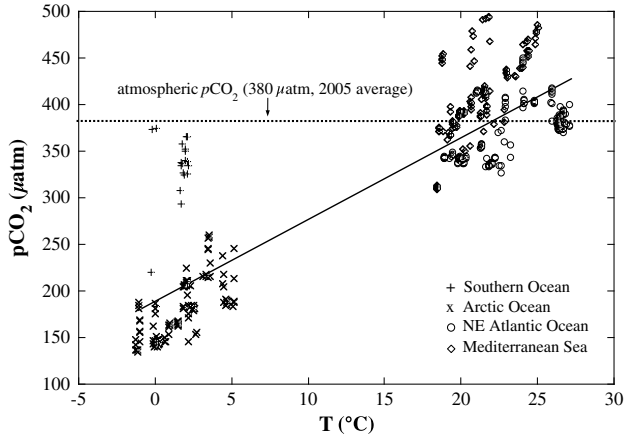

Figure 4. Relationship between seawater pCO_2 (µatm) and temperature (°C), for the whole data set: Southern Ocean (+), Arctic Ocean (x), North East Atlantic Ocean (○), and Mediterranean Sea (◊). The solid line represents the fitted linear regression equation $pCO_{2,T}$ (µatm) = 190 (±4) + 8.77 (±0.23) T (°C), $R^2 = 0.77$, $P < 0.0001$. The dashed line represents de mean value of atmospheric pCO_2 for the year 2005 (from Mauna Loa records), the middle year for our data set range (2003–2007).

[21] The range of variability of the difference between the pCO_2 at the top centimeters and at 5 m was quite substantial for pCO_2 (12.6 ± 1.4 µatm) and the maximum vertical difference reached 63 µatm (Figure 2b). Oxygen concentration within this layer also showed considerable vertical variability within stations (6.7 ± 1.0 µmol O_2 Kg^{-1}), and the maximum difference observed at any one station was −67.3 µmol O_2 Kg^{-1} (Figure 2c). In polar waters, the most productive areas during spring-summer, when sampling was performed, a clear relationship between vertical changes in O_2 and pCO_2 was observed (Figures 2b and 2c). Southern waters presented generally lower pCO_2 values at the top centimeters than at 5–8 m below. Accordingly, the upper centimeters of the water column were generally higher in O_2 evoking community metabolism to be exerting a strong control on vertical CO_2 variability among those meters and suggesting a net enrichment in microautotrophs in the very top of the water column fixing CO_2 at higher rates than those from a few meters below in Antarctic waters. On the contrary, we observed the Arctic Ocean to show a general increase in pCO_2 and decrease in O_2 concentrations in the top centimeters when compared to those from a few meters below, suggesting a heterotrophic enrichment activity in the top centimeters in those waters.

[22] Among the overall data set, pCO_2 and oxygen concentration values differed systematically, but not consistently, between the top centimeters and 5 m depth, showing almost all possible profiles (see Figure 3 for some examples, and Figure S1 in the supporting information for all profiles) revealing either metabolic effects driving pCO_2 vertical variability with nonsignificant changes in temperature in the NE Atlantic and Southern Ocean (Figures 3a, 3b and 3e, 3f, respectively), or the biological and thermodynamic effect driving pCO_2 changes towards the same direction in the Mediterranean Sea and the Arctic Ocean (Figures 3c, 3d and 3g, 3h respectively). Note that those are just examples and do not represent general patterns of any of the studied areas.

3.2. Controls of pCO_2 Vertical Variability in the Upper Meters of the Ocean

[23] On a global scale, and considering all data collected, pCO_2 correlated strongly with water temperature. The dependency of pCO_2 with water temperature ($pCO_{2\ T}$) is described by the following equation: $pCO_{2\ T}$ (µatm) = 190 (±4) + 8.77 (±0.23) T (°C) [$R^2 = 0.77$, $P < 0.0001$, see Figure 4], with pCO_2 values doubling for every 21°C temperature increase ($\partial \ln pCO_2/\partial T = 0.0324°C^{-1}$). This relationship exhibits less increase than that established by *Takahashi et al.* [1993] for isochemical seawater conditions, where pCO_2 values double every 16°C ($\partial \ln pCO_2/\partial T = 0.0423°C^{-1}$), meaning that the sum of other effects is counteracting the pCO_2 increase expected by T changes alone. In contrast, oxygen concentrations were independent ($P > 0.05$) of temperature changes. We observed that pCO_2 strongly correlated with absolute latitude ($R^2 = 0.70$, $P < 0.0001$) presenting lower values at polar productive cold waters and higher values at subtropical oligotrophic warm waters.

[24] To evaluate the biological effect on changes in pCO_2, we removed the temperature effect by normalizing the pCO_2 observed values ($pCO_{2\ obs}$) to a constant temperature of 15.9°C, the mean surface temperature for our data set (T_{mean}), using the equation proposed by *Takahashi et al.* [1993, 2002]: $pCO_2\ (T_{mean}) = pCO_{2obs}\ e^{0.0423\ (Tmean-Tobs)}$, where pCO_2 (T_{mean}) is the pCO_2 normalized to the mean surface Temperature (T_{mean}), and T_{obs} is the temperature observed or measured in situ. The dependency of pCO_2 (T_{mean}) with changes in O_2 concentration was then analyzed for the different studied areas. We found pCO_2 (T_{mean}) to be significantly and negatively correlated with changes in O_2 concentration when considering all data from polar latitudes (from the Arctic and Southern Oceans) and the Mediterranean Sea [pCO_2 (T_{mean}) (µatm) = 1771 (±131) − 5.5 (±0.5) O_2 (µmol

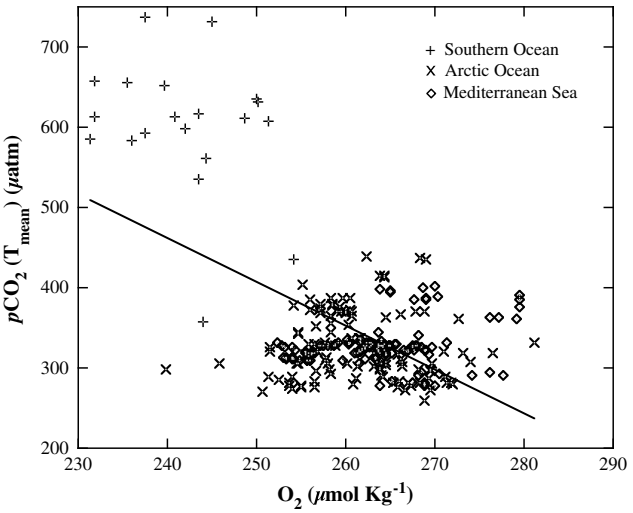

Figure 5. Relationship between seawater pCO_2 normalized to the mean temperature of 15.9°C (pCO_2 (T_{mean}) (µatm)) and oxygen concentration (µmol Kg^{-1}), considering all data from the Southern Ocean (+), Arctic Ocean (x), and Mediterranean Sea (◊). The solid line represents the fitted linear regression equation pCO_2 (T_{mean}) (µatm) = 1771 (±131) − 5.5 (±0.5) O_2 (µmol Kg^{-1}), $R^2 = 0.31$, $P < 0.0001$.

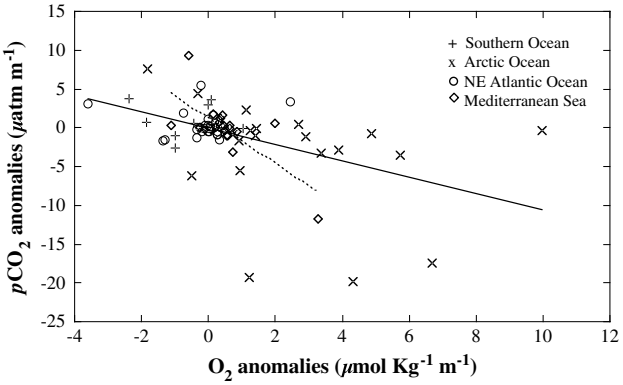

Figure 6. Relationship between vertical pCO_2 and O_2 concentration anomalies (in µatm m^{-1} and µmol Kg^{-1} m^{-1}, respectively) relative to temperature changes observed within the upper 5 m of the surface ocean. The solid line represents the fitted linear regression equation pCO_2 anomalies (µatm m^{-1}) = −0.02 (±0.51) − 1.05 (±0.24) O_2 anomalies (µmol Kg^{-1} m^{-1}), $R^2 = 0.21$, $P < 0.0001$, corresponding to all data set correlation. The dashed line represents the fitted linear regression equation pCO_2 anomalies (µatm m^{-1}) = 1.29 (±0.65) − 2.9 (±0.66) × O_2 anomalies (µmol Kg^{-1} m^{-1}), $R^2 = 0.52$, $P < 0.0001$, corresponding to data from the Mediterranean Sea.

Kg^{-1}), $R^2 = 0.31$, $P < 0.0001$, $N = 266$] (Figure 5). The changes in oxygen concentration explained more than 30% of the temperature-normalized pCO_2. When considering only polar data (exceeding 60°N and 60°S), a similar and even stronger dependency is found [pCO_2 (T_{mean}) (µatm) = 2374 (±190) −7.8 (±0.7) O_2 (µmol Kg^{-1}), $R^2 = 0.46$, $P < 0.0001$, $N = 136$]. As expected, higher oxygen values were associated with lower pCO_2 values than those expected by temperature, due to higher photosynthetic rates, while lower oxygen values are associated with increased pCO_2, reflecting higher net community respiration rates. The magnitude of that effect is amplified at polar latitudes, where an increase in oxygen of 20 µmol Kg^{-1} was associated with a drawdown of 150 µatm in surface pCO_2, whereas in the Mediterranean Sea, the same oxygen change was associated with a biological pCO_2 drawdown of 14 µatm, hence suggesting a lower capacity for biological CO_2 drawdown at warm subtropical latitudes than at high polar latitudes. Similar effects were observed by Takahashi and co-workers [1993, 2002], who postulated biological effects on oceanic pCO_2 at high latitudes to exceed 140 µatm and to be around 50 µatm in subtropical and tropical latitudes; however, data from the Mediterranean Sea was lacking in their data set.

[25] On the other hand, data collected in the North East Subtropical Atlantic presented lower pCO_2 (T_{mean}) and they do not significantly correlate with oxygen concentration, probably due to low primary production in these nutrient-depleted waters. However, pCO_2 (T_{mean}) did positively and significantly correlate with distance to the coast, represented by longitude (°W), [$R^2 = 0.62$, $P < 0.0001$, $N = 158$] exhibiting an increase in sea surface pCO_2 magnitude and variability towards the North West African coast due to the monsoon-induced upwelling of deep waters in this coastal area.

[26] The role of temperature variability on the observed vertical variability in pCO_2 and O_2 concentration was further investigated by taking pCO_2 at 5 m depth (or the highest depth sampled, between 3 and 8 m, when 5 m depth data was not recorded) and calculating the corresponding values expected at other depths from the observed T_{obs}. That was done using the corresponding temperature dependence equation for pCO_2 ($\delta \ln pCO_2/\delta T = 0.0423$°C, pCO_2 (expected at T_{obs}) = pCO_2 (at 5 m) $e^{0.0423\ (Tobs-T5m)}$) [*Takahashi et al.*, 1993]. Vertical variability in O_2 concentration expected by the observed temperature was also investigated by using the corresponding temperature dependence equation for O_2 [*Benson and Krause*, 1984]. The observed variability of temperature-corrected pCO_2 and temperature-corrected O_2 concentration within each profile averaged 10 ± 1 µatm of CO_2 and 5.1 ± 0.8 µmol O_2 Kg^{-1}, both significantly greater than 0 (*t* test, $P < 0.001$), confirming temperature-independent variability in pCO_2 and O_2 concentration within the upper meters of the ocean.

[27] Temperature variability within the upper 5 m accounted for (mean ± SE) 11 ± 3% and 9 ± 2% of the variance in pCO_2 and O_2 across stations, respectively, indicating that most of the vertical gas variability was caused by changes other than those in temperature. There was no significant relationship between the changes in wind velocity and the pCO_2 variability within the upper 5 m across stations ($P > 0.05$). Moreover, substantial variability in pCO_2 and O_2 within the top 5 m was observed even at moderate to high wind velocities (see Figures 3a, 3b, 3e, and 3f).

[28] To confirm that temperature is not the main process controlling pCO_2 vertical variability within the upper meters of the ocean, the relationship between the vertical pCO_2 and O_2 concentration anomalies, as the deviations from the values expected from temperature differences, were examined as a proxy to test the possible metabolic basis of pCO_2 vertical variability within the top meters. That was done by analyzing the differences between the observed pCO_2 and O_2 concentration changes with depth [$\Delta pCO_{2\ observed}/\Delta$depth and $\Delta O_{2\ observed}/\Delta$depth], and the temperature predicted pCO_2 and O_2 concentration changes with depth [$\Delta pCO_{2\ T}/\Delta$depth and $\Delta O_{2\ T}/\Delta$depth], where $pCO_{2\ T}$ and $\Delta O_{2\ T}$ are calculated by using *Takahashi et al.* [1993] and *Benson and Krause* [1984] equations, respectively. Vertical pCO_2 anomalies (in µatm m^{-1}) are then calculated as [$\Delta pCO_{2\ observed}/\Delta$depth] − [$\Delta pCO_{2\ T}/\Delta$depth] and O_2 anomalies (in µmol Kg^{-1} m^{-1}) are calculated as [$\Delta O_{2\ observed}/\Delta$depth] − [$\Delta O_{2\ T}/\Delta$depth]. The pCO_2 and O_2 anomalies negatively and significantly correlated ($R^2 = 0.21$, $P < 0.001$) (see solid line in Figure 6) when analyzing all profiles together. We found this correlation between pCO_2 and O_2 anomalies to be similar for polar waters ($R^2 = 0.17$, $P < 0.05$) and much stronger in the Mediterranean Sea, when excluding the Black Sea, ($R^2 = 0.52$, $P < 0.001$) (see dashed line in Figure 6). However, the vertical O_2 concentration range in the measured profiles of the Mediterranean Sea shows smaller values (3.4 ± 0.5 µmol O_2 Kg^{-1}) than those observed at high-latitude polar waters (7.3 ± 1.5 µmol O_2 Kg^{-1}). Altogether, our data display evidence of metabolic changes occurring in the top meters of the ocean that significantly control the vertical anomalies in CO_2 observed within this surface layer, explaining more than 50% of the pCO_2 anomalies observed in the Mediterranean Sea. On the other hand, data collected on the North East subtropical Atlantic presents lower pCO_2 vertical anomalies than those in the Mediterranean and polar waters and they do not significantly correlate with oxygen anomalies.

Table 2. Summary of Selected Biological and Chemical Parameters (Average ± SE): Bacterial Respiration (BR) in μmol O_2 L^{-1} d^{-1}, Dissolved Organic Nitrogen (DON) in μmol L^{-1}, Total Hydrolizable Amino Acid Concentration (THAA) in μmol L^{-1}, and Dissolved Organic Carbon (DOC) in μmol L^{-1}, in the Surface Microlayer (SML) and the Underwater Layer (UWL), for two of the Studied Geographical Regions[a]

	BR(μmol O_2 L^{-1} d^{-1})		DON(μmol L^{-1})		THAA(μmol L^{-1})		DOC(μmol L^{-1})	
Geographical Region	SML	UWL	SML	UWL	SML	UWL	SML	UWL
NE Subtropical Atlantic								
COCA-2 [*Calleja et al*., 2005, 2009]	6.7 ± 1.9	2.2 ± 0.9					110 ± 5	76 ± 6
BADE-2 [*Reinthaler et al*., 2008]	7.5 ± 1.6	0.8 ± 0.8	18.3 ± 1.9	5.5 0.2	5.45 ± 1.43	0.45 ± 0.02	161 ± 24	111 ± 17
Southern Ocean								
ICEPOS [*Calleja et al*., 2009]							70 ± 4	55 ± 2

[a]SML in *Reinthaler et al*. [2008] represents the top 40–80 μm surface layer, while SML in *Calleja et al*. [2005, 2009] represents the top 2 cm layer. UWL in *Reinthaler et al*. [2008] represents water sampled at around 30–50 m depth, while ULW in *Calleja et al*. [2005, 2009] represents water sampled from 5 m depth.

[29] Overall, the small temperature vertical changes observed within this study were comparable to those reported in the past [*Donlon et al*., 2002; *Fairall et al*., 1996; *Gemmrich and Farmer*, 1999; *Ward et al*., 2004] and accounted for less than 20% of the observed vertical pCO_2 variability. This suggests the strong influence of biological activity contributing to changes in pCO_2 within the upper meters of the surface ocean, which is supported by the biological and chemical data available from three of the same cruises where this study was conducted (COCA-2 [*Calleja et al*., 2005, 2009], BADE-2 [*Reinthaler et al*., 2008], and ICEPOS [*Calleja et al*., 2009]). This data, shown in Table 2, revealed that the surface microlayer was significantly enhanced in microbial respiration rates (by a factor of 3 to 9) and dissolved organic carbon (DOC) concentrations (by 25–45%). A consistent and pronounced enrichment was also observed on the concentration of Dissolved Organic Nitrogen (of a factor of more than 3) and of total hydrolizable amino acids (THAA), a major carbon and energy sources for marine microbes [*Keil and Kirchman*, 1992] that showed differences of one order of magnitude within 1 m of the water surface [*Reinthaler et al*., 2008].

[30] The observed prevalence of negative relationships between the deviations of pCO_2 and O_2 concentration from the values expected from temperature variability further suggest biological processes as key drivers of the observed pCO_2 heterogeneity. These results are in accordance with the mentioned data showing that the top centimeters of the ocean support metabolic rates far greater than the waters at 5 m depth [*Calleja et al*., 2005; *Reinthaler et al*., 2008] and directly affect air-sea pCO_2 gradients. The evidence of strong biologically driven pCO_2 and O_2 concentration changes within the upper meters of the ocean suggest that metabolic effects on pCO_2 changes could be often faster than mixing time scales, reported to vary between 0.5 h and hundreds of hours [*Denman and Gargett*, 1983], hence allowing these heterogeneities to persist in the presence of mixing.

4. Concluding Remarks

[31] Our results show the prevalence of substantial variability in pCO_2 (averaging 12.6 ± 1.4 μatm and reaching a maximum value of 63 μatm) within the upper several meters of the open ocean in all the areas sampled. This contrasts with the assumed homogeneity in pCO_2 within the top meters of the ocean, implicit in conventional survey programs [*Fung and Takahashi*, 2000; *Takahashi et al*., 2002, 2009] and inherent to most applications, as routine and conventional sampling instruments (e.g., CTD-Rosette sampling systems) cannot properly resolve the top meter of the ocean, where sensors are affected by ship motion. The assumed homogeneity of pCO_2 within the upper several meters of the open ocean has led international efforts to improve CO_2 flux estimates to target improvement in the precision and accuracy of analytical systems [*Körtzinger et al*., 2000], quality control of the integrated data bases [*Pfeil et al*., 2013], and parameterization of the gas exchange coefficient [*Wanninkhof et al*., 2009] as key actions. However, our results provide ample evidence for the prevalence of substantial heterogeneity in pCO_2 within the top meters of the ocean. The evidence presented here should prompt efforts to resolve and understand departures from the assumption of pCO_2 vertical homogeneity within that surface layer, as it can constitute a significant source of error in both the magnitude and the direction of air-sea CO_2 flux estimates. By adding the mean difference between the surface water pCO_2 at 0 and 5 m from our measurements to the Takahashi's climatology air-sea CO_2 gradient, referred to the year 2000 [*Takahashi et al*., 2009], we have calculated the new net air-sea flux at the overlapping grid points and months (see Table S1 in the supporting information for a detailed explanation of the calculations). The results estimate that the Arctic Ocean would be a stronger CO_2 sink (up to 3.5 times higher) and the Southern Ocean would be a more moderate CO_2 sink than that predicted by Takahashi. On the other hand, the North East subtropical Atlantic does not seem to show a clear trend (see Table S1).

[32] In summary, the data presented here clearly indicates that the top meters of the ocean is an area far more dynamic and heterogeneous in metabolic gases than hitherto considered. This heterogeneity and the combination of physical and biological processes driving it should be further investigated to adequately improve our understanding of air-sea CO_2 exchange and accurately assess the global oceanic uptake of atmospheric CO_2.

[33] **Acknowledgments.** This research was funded by the projects COCA (REN-2000-1471-C02), RODA (CTM-2004-06842-CO3-O2), BADE (REN-2002-12284E/MAR, NWO-ALW 812.03.001), ICEPOS (REN2002-04165-CO3-O2), THRESHOLDS (CTM2005-24238-E/MAR), ATOS (POL2006-00550/CTM), the MALASPINA 2010 Expedition (CSD2008-00077), R + D National Plan of the Spanish Ministry of Science and Innovation, and the Dutch Earth and Life Sciences. We thank the crew of the R/V Hespérides, R/V Pelagia, R/V García del Cid, and the UTM personnel for their assistance. M.Ll.C was supported by the Spanish Research

council [CSIC, grant JAEDOC030, co-funded by the Fondo Social Europeo (FSO)] and the Agency for Administration of University and Research Grants (AGAUR, grant 2007 BP-A 00156). M.A. was funded by grant ORCASEX (RYC-2006-001836). R.V.-S. was funded by THRESHOLDS integrated project (003933–2).

Reference

Agogué, H., F. Joux, I. Obernosterer, and P. Lebaron (2005), Resistance of marine bacterioneuston to solar radiation, *Appl. Environ. Microbiol.*, *71*(9), 5282–5289.

Benson, B. B., and D. Krause Jr. (1984), The concentration and isotopic fractionation of oxygen dissolved in fresh water and seawater in equilibrium with the atmosphere, *Limnol. Oceanogr.*, *29*, 620–632.

Calleja, M. Ll., C. M. Duarte, N. Navarro, and S. Agustí (2005), Control of air-sea CO_2 disequilibria in the subtropical NE Atlantic by planktonic metabolism under the ocean skin, *Geophys. Res. Lett.*, *32*, L08606, doi:10.1029/2004GL022120.

Calleja, M. Ll., C. M. Duarte, Y. T. Prairie, S. Agustí, and G. J. Herndl (2009), Evidence for surface organic matter modulation of air-sea CO_2 gas exchange, *Biogeosciences*, *6*, 1105–1114.

Corbière, A., N. Metzl, G. Reverdin, C. Brunet, and T. Takahashi (2007), Interannual and decadal variability of the oceanic carbon sink in the North Atlantic subpolar gyre, *Tellus Series B, Chem. Phys. Meteorol.*, *59*(2), 168–178.

Cunliffe, M., A. Engel, S. Frka, B. Gašparovic, C. Guitart, J. C. Murrell, M. Salter, C. Stolle, R. Upstill-Goddard, and O. Wurl (2013), Sea surface microlayers: A unified physicochemical and biological perspective of the air–ocean interface, *Prog. Oceanogr.*, *109*, 104–116.

Denman, K. L., and A. E. Gargett (1983), Time and space scales of vertical mixing and advection of phytoplankton in the upper ocean, *Limnol. Oceanogr.*, *28*(5), 801–815.

Donlon, C. J., P. J. Minnett, C. Gentemann, T. J. Nightingale, I. J. Barton, B. Ward, and M. J. Murray (2002), Toward improved validation of satellite sea surface skin temperature measurements for climate research, *J. Clim.*, *15*, 353–369.

Ducklow, H. W., and S. L. McCallister (2004), The biogeochemistry of carbon dioxide in the coastal oceans, in *The Sea*, vol. 13, edited by A. R. Robinson et al., pp. 269–315, Harvard University Press, Cambridge, MA.

Fairall, C. W., E. F. Bradley, J. S. Godfrey, G. A. Wick, J. B. Edson, and G. S. Young (1996), Cool-skin and warm-layer effects on sea surface temperature, *J. Geophys. Res.*, *101*(C1), 1295–1308.

Franklin, M. P., I. R. McDonald, D. G. Bourne, N. J. P. Owens, R. C. Upstill-Goddard, and J. C. Murrell (2005), Bacterial diversity in the bacterioneuston (sea surface microlayer): The bacterioneuston through the looking glass, *Environ. Microbiol.*, *7*, 723–736.

Fung, I., and T. Takahashi (2000), Estimating air-sea exchanges of CO_2 from pCO_2 gradients: Assessment of uncertainties, in *The Carbon Cycle*, edited by T. M. L. Wigley and D. S. Schimel, pp. 125–133, Cambridge Univ. Press, Cambridge.

Fung, I. Y., S. C. Doney, K. Lindsay, and J. John (2005), Evolution of carbon sinks in a changing climate, *Proc. Natl. Acad. Sci. U. S. A.*, *202*, 11,201–11,206, doi:10.1073/pnas.0504949,102.

Gemmrich, J. R., and D. M. Farmer (1999), Near-surface turbulence and thermal structure in a wind driven sea, *J. Phys. Oceanogr.*, *29*, 480–499.

Gong, H., Z. Zhengbin, C. Zhang, L. Liu, and L. Xing (2007), Multilayer distribution of carbon dioxide system in surface water of the Yellow Sea in spring, *Chin. J. Oceanol. Limnol.*, *25*(1), 1–15.

Gruber, N., et al. (2009), Oceanic sources, sinks, and transport of atmospheric CO_2, *Global Biogeochem. Cycles*, *23*, GB1005, doi:10.1029/2008GB003349.

Hari, P., J. Pumpanen, J. Huotari, P. Kolari, J. Grace, T. Vesala, and A. Ojala (2008), High-frequency measurements of productivity of planktonic algae using rugged nondispersive infrared carbon dioxide probes, *Limnol. Oceanogr. Methods*, *6*, 347–354.

Hartman, B., and D. E. Hammond (1985), Gas exchange in San Francisco Bay, *Hydrobiologia*, *129*, 59–68.

Inoue, H. Y., M. Ishii, H. Matsueda, M. Ahoyama, and I. Asanuma (1996), Changes in longitudinal distribution of the partial pressure of CO_2 (pCO_2) in the central and western equatorial Pacific, west of 160°W, *Geophys. Res. Lett.*, *23*(14), doi:10.1029/96GL01674.

Joux, F., H. Agogué, I. Obernosterer, C. Dupuy, T. Reinthaler, G. J. Herdnl, and P. Lebaron (2006), Microbial community structure in the sea surface microlayer at two contrasting coastal sites in the northwestern Mediterranean Sea, *Aquat. Microb. Ecol.*, *42*, 91–104.

Keil, R. G., and D. L. Kirchman (1992), Bacterial hydrolysis of protein and methylated protein and its implications for studies of protein degradation in aquatic systems, *Appl. Environ. Microbiol.*, *58*, 1374–1375.

Körtzinger, A., et al. (2000), The international at-sea intercomparison of *f*CO2 systems during the R/V Meteor cruise 36/1 in the North Atlantic Ocean, *Mar. Chem.*, *72*, 171–192.

Le Quéré, C., T. Takahashi, E. T. Buitenhuis, C. Rödenbeck, and S. Sutherland (2010), Impact of climate change and variability on the global oceanic sink of CO_2, *Global Biogeochem. Cycles*, *24*, GB4007, doi:10.1029/2009GB003599.

Liu, C., C. Zhang, X. Yang, H. Gong, and Z. Zhang (2008), A multilayer study of pCO_2 in the surface waters of the Yellow and South China Seas in spring and the sea-air carbon dioxide flux, *J. Ocean Univ. China*, *7*(3), 263–268, doi:10.1007/s11802-007-0263-2.

Lüger, H., D. W. R. Wallace, A. Ko¨rtzinger, and Y. Nojiri (2004), The pCO_2 variability in the mid latitude North Atlantic Ocean during a full annual cycle, *Global Biogeochem. Cycles*, *18*, GB3023, doi:10.1029/2003GB002200.

McKinley, G. A., A. Fay, T. Takahasi, and N. Metzl (2011), Convergence of atmospheric and North Atlantic CO_2 trends on multidecadal timescales, *Nat. Geosci.*, doi:10.1038/ngeo1193.

Metzl, N., A. Poisson, F. Louanchi, C. Brunet, B. Schauer, and B. Bres (1995), Spatio-temporal distributions of air-sea fluxes of CO_2 in the Indian and Antarctic oceans, *Tellus Series B Chem. Phys. Meteorol.*, *47*(1–2), 56–69, doi:10.1034/j.1600-0889.47.issue1.7.x.

Murphy, P. P., Y. Nojiri, Y. Fujinuma, C. S. Wong, J. Zeng, T. Kimoto, and H. Kimoto (2001), Measurements of surface sea water fCO_2 from volunteer commercial ships: Techniques and experiences from Skaugran, *J. Atmos. Oceanic Technol.*, *18*, 1719–1734.

Obernosterer, I., P. Catala, T. Reinthaler, G. J. Herndl, and P. Lebaron (2005), Enhanced heterotrophic activity in the surface microlayer of the Mediterranean Sea, *Aquat. Microb. Ecol.*, *39*, 293–302.

Parsons, T. R., Y. Maita, and C. M. Lalli (1984), *A manual of chemical and biological methods for sea water analysis*, Pergamon Press, Oxford.

Pfeil, B., et al. (2013), A uniform, quality controlled Surface Ocean CO_2 Atlas (SOCAT), *Earth Syst. Sci. Data*, *5*(1), 125–143, doi:10.5194/essd-5-125-2013.

Phillips, L. F. (2004), The role of the air-sea temperature difference in air-sea exchange, *Geophys. Res. Lett.*, *31*, L17301, doi:10.1029/2004GL020699.

Reinthaler, T., E. Sintes, and G. J. Herndl (2008), Dissolved organic matter and bacterial production and respiration in the sea-surface microlayer of the open Atlantic and the western Mediterranean Sea, *Limnol. Oceanogr.*, *53*, 122–136.

Robertson, J. E., and A. J. Watson (1992), Thermal skin effect of the surface ocean and its implications for CO_2 uptake, *Nature*, *358*, 738–740.

Santana-Casiano, J. M., M. González-Dávila, and I. R. Ucha (2009), Carbon dioxide fluxes in the Benguela upwelling system during winter and spring: A comparison between 2005 and 2006, *Deep Sea Res., Part II*, *56*(8–10), 533–541.

Takahashi, T., J. Olafsson, J. G. Goddard, D. W. Chipman, and S. C. Sutherland (1993), Seasonal variation of CO_2 and nutrients in the high-latitude surface oceans: A comparative study, *Global Biogeochem. Cycles*, *7*(4), 843–878.

Takahashi, T., et al. (2002), Global sea-air CO_2 flux based on climatological surface ocean pCO_2, and seasonal biological and temperature effects, *Deep Sea Res., Part II*, *49*, 1601–1622.

Takahashi, T., et al. (2009), Climatological mean and decadal change in surface ocean pCO_2, and net sea–air CO_2 flux over the global oceans, *Deep Sea Res., Part II*, *56*, 554–577.

Takahashi, T., S. C. Sutherland, and A. Kozyr (2012), Global ocean surface water partial pressure of CO_2 database: Measurements performed during 1957–2011 (version 2011). ORNL/CDIAC-160, NDP-088(V2011). Carbon Dioxide Information Analysis Center, Oak Ridge National Laboratory, U.S. Department of Energy, Oak Ridge, Tennessee, doi:10.3334/CDIAC/OTG.NDP088(V2011).

Wanninkhof, R., W. E. Asher, D. T. Ho, C. Sweeney, and W. R. McGillis (2009), Advances in quantifying air-sea gas exchange and environmental forcing, *Annu. Rev. Mar. Sci.*, *1*, 213–244.

Ward, B., R. Wanninkhof, W. R. McGillis, A. T. Jessup, M. D. DeGrandpre, J. E. Hare and J. B. Edson (2004), Biases in the air-sea flux of CO2 resulting from ocean surface temperature gradients, *J. Geophys. Res.*, *109*, C08S08, doi:10.1029/2003JC001800.

Weiss, R. F. (1974), Carbon dioxide in water and seawater: The solubility of a non-ideal gas, *Mar. Chem.*, *2*, 203–215.